Journal Pre-proof

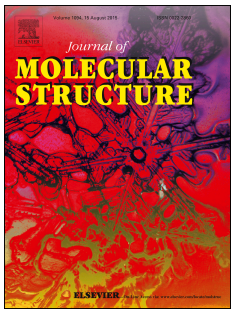

Novel Mn^{2+}, Fe^{3+}, Co^{2+}, Ni^{2+} and Cu^{2+}complexes of potential OS donor thiosemicarbazide: Design, structural elucidation, anticorrosion potential study and antibacterial activity

Ola A. El-Gammal, Abd El-Aziz S. Fouda, Doha M. Nabih

PII: S0022-2860(19)31604-7

DOI: https://doi.org/10.1016/j.molstruc.2019.127495

Reference: MOLSTR 127495

To appear in: *Journal of Molecular Structure*

Received Date: 28 August 2019

Revised Date: 21 November 2019

Accepted Date: 27 November 2019

Please cite this article as: O.A. El-Gammal, A.E.-A.S. Fouda, D.M. Nabih, Novel Mn^{2+}, Fe^{3+}, Co^{2+}, Ni^{2+} and Cu^{2+}complexes of potential OS donor thiosemicarbazide: Design, structural elucidation, anticorrosion potential study and antibacterial activity, *Journal of Molecular Structure* (2019), doi: https://doi.org/10.1016/j.molstruc.2019.127495.

Graphical Abstract

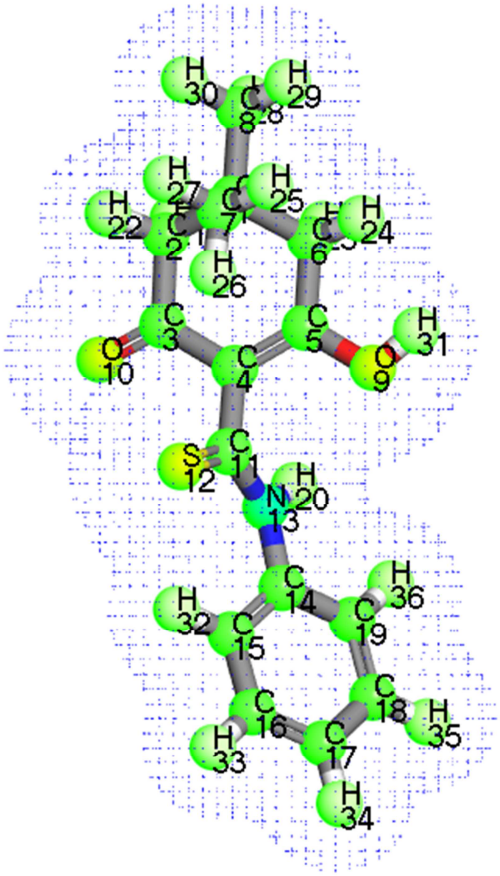

Electron density for HDDPT

Novel Mn^{2+}, Fe^{3+}, Co^{2+}, Ni^{2+} and Cu^{2+}complexes of potential OS donor thiosemicarbazide: Design, structural elucidation, anticorrosion potential study and antibacterial activity

Ola A. El-Gammal*, Abd El-Aziz S. Fouda and Doha M.Nabih

Chemistry Department; Faculty of Science; Mansoura University- Mansoura, P.O; 70, Mansoura; Egypt

Abstract

Novel series of Co^{2+}, Ni^{2+}, Cu^{2+}, Mn^{2+} and Fe^{3+}complexes derived from 4,4-dimethyl-2,6-dioxo-N-phenylcyclohexanecarbothioamide (HDDPT) were prepared and characterized by conventional techniques. The complexes have adopted the formulae; {[Mn(DDPT)Cl($H_2O)_3$].$3H_2O$, [Ni(DDPT-H)(H_2O)(OH)], [Cu (HDDPT) $Cl_2(H_2O)_2$].$2H_2O$, [$Co(HDDPT)_2Cl_2$] and [Fe (DDPT)Cl_2] , respectively. Spectral data revealed that HDDPT coordinates as OS donor in a neutral or mononegative manner. Electronic and magnetic measurements suggested a square planar geometry for Ni^{2+} complex and an octahedral one for the other complexes. X-ray powder diffraction data suggested monoclinic and orthorhombic structures for Fe^{3+} and Ni^{2+}complexes, respectively. DFT method was utilized to prove the geometry and evaluate the bond lengths, bond angles as well as different energetic parameters. The thermal stability of the compounds was examined and the corresponding thermodynamic parameters were determined using Coats-Redfern and Horowitz-Metzger methods. Also, the corrosion hindrance of carbon steel (CS) in 0.5M HCl by HDDPT was carried out using potentiodynamic polarization (PP) measurement. The data proved the thiosemicarbazide to be a powerful inhibitor and it is demonstrated that the protection efficiency and surface converge (Ɵ) increase with increasing the inhibitor concentration and decrease with increasing temperature. Finally, the adsorption procedure obeys Langmuir's adsorption isotherm. Moreover, all compounds were screened against the growth of four pathogenic bacterial strains.

Keywords: OS bidentate, thermodynamic parameters, orthorhombic, corrosion of carbon steel.

*Corresponding author: e-mail: olaelgammal@yahoo.com Tel: 002-01018199550

1. Introduction

Over decades, thiosemicarbazides are proved to be potent intermediates for the synthesis of numerous pharmaceutical and bioactive materials and thus, they are utilized extensively in medicinal chemistry. The diversity of heterocycles generated from thiosemicarbazides is associated primarily with the fact that these compounds can exhibit properties of N(1)-; N(2)-; N(1);N(4)-; N(2);N(4)-;

N(1);S-, N(2);S- and N(4),S-nucleophiles [1].Also, thiosemicarbazides have been extensively utilized commercially as dyes, photographic films, plastic and in textile industry[2]. Transition metal complexes derived from thiosemicarbazides become of valuable importance in industry and biology[3].Such metal complexes have revealed obviously the role played by sulfur coordination in these compounds and consequently their "soft by acid-soft base" preference is [4].The real impetus toward developing the coordination chemistry of these potential ligands was probably provided by the remarkable antitumor [5], antiviral [6], and antimalarial [7,8] activity observed for some of these derivatives, which has since been shown to be related to their metal-complexing ability [9]. Obviously, the molecular features essential for such activities must be ascertained by designing synthetic routes to modify, replace, or substitute the derived thiosemicarbazide. Thus, as part of a research programme aimed at the synthesis of compounds with antibacterial, antioxidant and antitumor properties,[10-14] we prepared and characterized new Co^{2+}, Ni^{2+}, Cu^{2+}, Mn^{2+} and Fe^{3+}complexes of 4,4-dimethyl-2,6-dioxo-N-phenylcyclohexanecarbothioamide (HDDPT).The word extended to include the test of the inhibition power of the thiosemicarbazide towards corrosion hindrance of carbon steel in 0.5M HCl as well as the antibacterial activity of all title compounds.

2. Experimental

2.1. Materials

All reagents used were purchased from Fluka, Aldrich-Sigma companies. For corrosion study, pipeline carbon steel (CS) according to the American Petroleum Institute (API) grade N80 (weight %; C=0.23, Mn=1.35, Cr=0.05, Mo=0.01, Si=0.22, P=0.017, S=0.01, Ni=0.02 & Fe=98.093) was utilized for corrosion study.

2.2. Instrumentation

Thermo-Nicolet IS10 FTIR spectrometer was used for IR spectral measurements (as KBr disc). Unicam UV-VIS UV2 spectrometer was used to measure the electronic spectra. ^{1}H-NMR spectra in d_6-DMSO was recorded on a Varian Gemini WM-200 MHz spectrometer. XRD patterns were recorded using Bruker aXS-D8 Advance Cu-Kα diffractometer (wavelength, λ = 1.504 Å). Thermogravimetric analysis performed using an automatic recording Thermo balance, type 951 DuPont; heating rate of 10 °C/min (25-800 °C) in N_2. Mass spectrum recorded on Varian Mat 311. Molar conductance (10^{-3} mol/l in DMF) was measured on a Tacussel conductivity bridge model CD6NG. The C, H, N and S contents, were determined using a Perkin-Elmer 2400 series II analyzer while M and Cl contents were determines according to standard method [15].

2.3 Preparation of HDDPT

0.7 g of 5,5-dimethyl 1,3-cyclohexandione (5mmol) were added to 0.6 ml of phenylisothiocyanate (5mmol) in presence of 0.28g solid KOH (5 mmol) and 15 ml DMF. The reaction mixture was heated under reflux with stirring overnight. Then poured in ice, two drops of concentrated hydrochloric acid were added and the pale yellow precipitate that formed was filtered off, washed several times with cold water and allowed to dry in a vacuum desiccator over anhydrous$CaCl_2$. The product was tested by TLC, IR and ^{1}HNMR and the yield was %80 (0.277 g); m.p.:130^{0}C.

2.4. Preparation of metal complexes

The metal chloride (1.0 mmol) in ethanol was added to ethanolic solution of HDDPT (0.2751 g,1 mmol) and heated under reflux for 2–3 h and the precipitates formed were filtered, washed with ethanol, diethyl ether and finally dried in a vacuum desiccator over anhydrous$CaCl_2$ and checked by TLC, partial elemental analysis (C, H, N and S) as well as spectral tools (IR, UV-Vis.,). The analytical data are listed in table 1 and the complexes are stable in air, soluble in dimethylformamide (DMF) and dimethyl sulfoxide (DMSO) and non-electrolytes (1-18 ohm^{-1} cm^2 mol^{-1}) [16]. Many trials were performed to isolate a single crystal but failed.

2.5. Corrosion study

2.5.1. Solutions

1 M solution of HCl (analytical Grade, 37%) was prepared by diluting it with bidistilled water in 1:2 acid to water ratio. A series of solutions of the inhibitor, namely HDDPT were prepared.

2.5.2. Corrosion measurements

The corrosion inhibition of CS in 1 M HCl in absence and presence of different doses of HDDPT has been investigated using potentiodynamic polarization (PP) measurement.

2.6. Antibacterial activity

The antibacterial activity of 200 mg/ml of HDDPT and its corresponding metal complexes in DMSO were carried out against *Streptococcus pyogenes ATCC 19615* and *Bacillus ATCC 6051* (Becton Dickinson and Company. Becton Dickinson Company, USA) as Gram-positive bacteria and *Klebsiella spp. 155095A (Carolina* trademark, USA) and *Escherichia Coli ATCC11775* as Gram-negative bacteria by agar well diffusion method [17].The positive control was ampicillin, ciprofloxacin and gentamicin drugs and DMSO was the negative one. The experiments were triplicate and the inhibition zone diameter was measured.

2.7. Molecular modeling

DMOL3 module calculations were used to examine the cluster estimations [18] and double numerical basis sets plus polarization functional (DNP) implemented in Materials Studio bundle [19]. It is designed for the realization of large scale density functional theory (DFT) calculations [20-23]. The geometric optimization is performed without any symmetry restriction.

3. Results and discussion

3.1. IR spectra

The most important IR bands of the ligand *viz* HDDPT and its metal complexes are listed in Table 2.The spectrum of the ligand shows strong bands at 1735 and 1661cm^{-1} assignable to stretching vibrations of hydrogen bonded and free carbonyl groups (Structure 1a) as revealed by a band at 3447 cm^{-1} (ν(OH)) and weak bands in the region 1800-1900 cm^{-1}. In complexes the ν (C=O) suffers weakness and shift to lower wavenumber suggesting, one of carbonyl groups converts to C-OH as supported by the new band 3447-3474 cm^{-1} [24] being not involved in chelation while the other participates in coordination. The bands due to thioamide I-IV vibrations observed at 1502, 1330 and 914 cm^{-1} which have substantial contributions from ν(C-N), δ(C-H) and δ (N-H) and vibrations [25].The band assigned to ν (NH) mode appeared at 3250 cm^{-1}. The stretching and bending vibrations (υ/ δ) of C=S group are observed as strong bands at 1277 and 785 cm^{-1}, respectively [26].The possibility of thione/thiol tautomerism in the solid state (Structure 1)is obscure as there are no bands characteristic for ν (SH) mode. On comparing the spectrum of and its metal complexes indicated that coordinates as OS neutral or monobasic chelate. Firstly, as neutral as in [Cu (HDDPT) Cl_2].4H_2O and [Co (HDDPT)$_2Cl_2$] (Structure 2a, 2c) *via* free (C=O) and C=S groups which confirmed by the shift of their bands to lower wavenumber. Secondly, HDDPT binds as monnegative bidentate in [Mn(DDPT)Cl($H_2O)_3$].3H_2O , [Fe (HDDPT) (DDPT)Cl_2] and [Ni(DDPT - H)($H_2O)_2$]complexes in thiol-enol form (Structures 2b, 2d and 2e) through C-S and the free C=O group as indicated by:

(i) The disappearance of bands due to υ/ δ(C=S) vibrations with simultaneous appearance of new bands at 1551 and 623 cm^{-1} assignable to new (C=N)*, resulting due to thiolization of (C=S) followed by deprotonation [27].

(ii) Shift of the band assigned to free (C=O) to lower wavenumber while the other one is converted into C-OH and does not participate in coordination as evidenced by the existence of the broad band at 3447 cm^{-1} [27], respectively (Structure 2).

(iii) The new bands at 524-504 cm^{-1} were observed and assigned to ν(M-O) vibration [27].

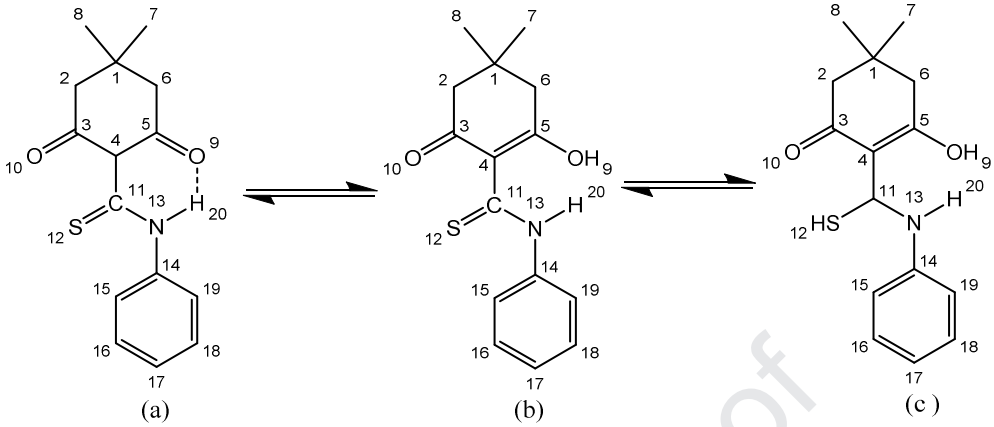

Structure 1:4,4-dimethyl-2,6-dioxo-N-phenylcyclohexanecarbothioamide (HDDPT).

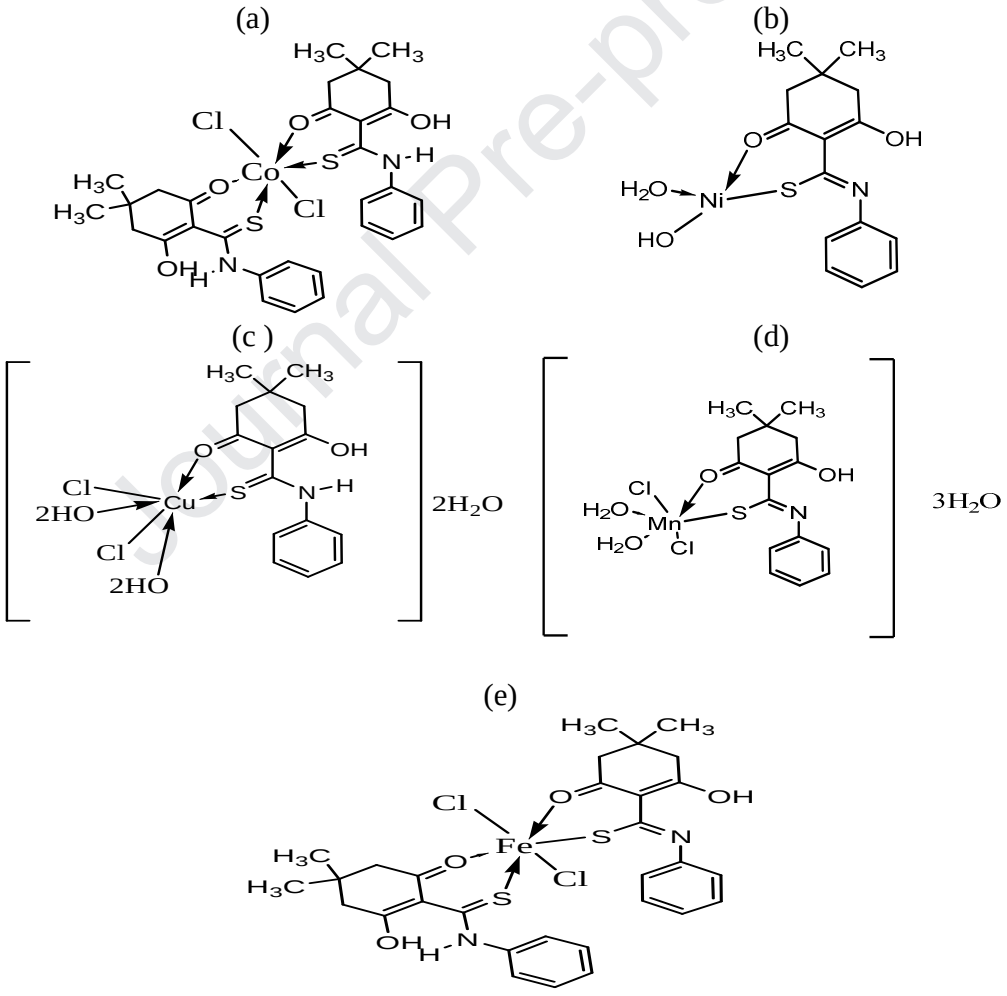

Structure 2:(a) $[Co(HDDPT)_2Cl_2]$, (b) $[Ni(DDPT)(OH)(H_2O)]$,(C) $[Cu(HDDPT)Cl_2(H_2O)_2].2H_2O$, (d) $[Mn(DDPT)Cl(H_2O)_3].3H_2O$ and (e) $[Fe(HDDPT)(DDPT)Cl_2]$.

3.2. ^{1}H, ^{13}C- NMR, spectra

The ^{1}H NMR spectrum of the ligand displayed ind6-DMSO (Fig. 1a) exhibits no signal in the region 8.00-11.00 ppm attributed to NH proton but instead two new signals at δ: 13.79 and 16.70 ppm appeared that may be referred to OH and SH protons resulting from rearrangement (Structure 1c) that disappeared upon adding D_2O confirming the possibility of thiol- enol form in solution. The signals attributable to phenyl protons appear as two multiplets at δ: 7.28-7.31 & 7.40-7.46 ppm. The peaks at 3.36 ppm (dd, J=7, 4H) and 1.01 ppm are due to the protons of two equivalent CH_2 groups (C2-C6) and $2CH_3$ protons. The^{13}C NMR spectrum of the ligand in d6-DMSO (Fig.1b) reveals signals at δ: 198.00, 188.30 and 137.30 ppm assignable to C-OH, C=O and (C-S), respectively [28]. The phenyl carbons appear as two multiplets at δ: 129.01-127.21 & 125.89-122.90 ppm. Moreover, the peaks for (C16-C17) and (C17-C18) appear as multiplet at 39.50 while that attributed to two C-C of unequivalent CH_2 groups appeared at 27.80 &27.30 ppm.

3.3. UV-visible spectra

The electronic absorption spectra were displayed in DMF and the data are represented in table 3. The bands that observed at 35530-32580.08 and 28370 cm^{-1} in the spectrum of HDDPT are due to (π→π*) and n → π*transitions [29] that suffer a noticeable great change upon complexation and appeared at 32980-30629 and 29841-26089 cm^{-1} indicating the chelation of central metal ion through the carbonyl and thione groups, respectively [30]. A new n→π* band at 19020-19626 cm^{-1} that overlap with $Cl\rightarrow M^{2+}$ transition was observed in the electronic spectra of the complexes confirming the coordination of S atom of C-S group to central metal ion.

The spectrum of Mn^{2+} complex showed bands at 26240, 19511 and 17552 assignable to $^{6}A_{1g}\rightarrow{}^{4}E_g(^{4}D)$, $^{6}A_{1g}\rightarrow{}^{4}T_{2g}(^{4}G)$ and $^{6}A_{1g}\rightarrow{}^{4}T_{1g}(^{4}G)$ transitions, respectively in an octahedral environment. The magnetic moment values (5.64 B.M.) is lower than the spin only value may be attributed to strong M-M interaction [31].

The spectrum of Fe^{3+} complex shows bands at 15608 and 24690 cm^{-1} assignable to $^{6}A_{1g}\rightarrow{}^{4}T_{1g}$(G)and $^{6}A_{1g}\rightarrow{}^{4}T_{2g}$ (G) transitions in an Oh configuration. The ν_3 corresponding to $^{6}A_{1g}\rightarrow{}^{4}E_g$ (G) not observed because it is covered by the broad ligand bands. Also, the band at 11764 cm-1 is referred to a low-energy thiolate→Fe (III) charge transfer band which causes a noticeable stability to iron in the +3 oxidation state [32]. In addition, the magnetic moment (4.26 B.M.) which is smaller

than the calculated value for two Fe (III) ions in octahedral geometries and this may be due to antiferromagnetism between the two ion-centers [33].

The electronic spectrum of Co^{2+} complex shows two bands at 15241 and 17136 cm^{-1} due to $^4T_{1g}(F) \rightarrow {}^4A_{2g}(F)$ (υ_2) and $^4T_{1g}(F) \rightarrow {}^4T_{1g}(P)$ (υ_3) transitions, respectively, in an octahedral configuration [34]. The calculated values of Dq, B and β and as well as the magnetic moment value μ_{eff} = 5.61 B.M. of the aforementioned complex lie in the range reported for octahedral Co (II) complexes [35].

The broad bands at 19626 (ν_2) and 23362 (ν_3) cm^{-1} are assignable to $^1A_{1g} \rightarrow {}^1A_{2g}$ transition and to spin-forbidden transition $^1A_{1g} \rightarrow {}^1B_{2g}$ in [Ni (DDPT) (H_2O) (OH)] complex [36] (fig.2) as well as the magnetic moment value ($\mu_{eff.}$ = zero) suggesting a square planar geometry.

Finally, the bands at 17376 and 18954 cm^{-1} assignable to $^2B1g \rightarrow {}^2Eg$ and $^2B_{1g} \rightarrow {}^2A_{1g}$ transitions in the spectrum of Cu^{2+} complex support an octahedral geometry. The band at 21186 cm^{-1} is referred to S→Cu transition [37]. Also, the magnetic moment value ($\mu_{eff.}$ =2.04 B.M.) is consistent with one unpaired electron [37].

3.4. Electron paramagnetic resonance

The EPR spectrum of powdered [Cu (HDDPT) Cl_2].$4H_2O$ complex (Fig.3) was recorded at room temperature. The spectrum is unique in that it can be directly correlated to the equatorial ligand types and is typical spectrum similar to those reported for mononuclear copper [38]. It exhibits a broad single line focused at g = 2.08 with well resolved hyperfine structure suggesting that the thiosemicarbazide (ONS) chelating system seems to be coplanar with the two chelate rings, thus adopting the nearly planar octahedral structure ($g_{\square\square\square}$(2.180)> $g_{\perp}$(2.088)).□ The interaction between Cu(II) ion and neighbors, expressed by G(2.07 < 4.0) indicates an appreciable exchange coupling present in solid complexes. The hyperfine splitting for parallel orientation value ($A_{\square\square\square\square}$=0.007) is larger than those for the perpendicular one ($A_{\perp}$=0.006) revealing that the single d electron is in a □-nonbonding orbital away from the equatorial plane ligands and consistent with the literature [39].The molecular orbital coefficient (α^2) for in-plane σ-bonding and β 2 (π-bonding) was calculated and found to be 0.44 and 0.97, respectively indicating that in-plane σ-bonding is more covalent and in a good agreement the literature [40].

3.5. Mass spectral studies

The mass spectra of all compounds were recorded and represented in figure 1S (Supplementary material). The spectrum of HDDPT showed the fragmentation patterns which is corresponding to degradation of the molecule the parent peak at m/z = 75.21(Calcd.275.10) corresponding to $C_{15}H_{17}O_2NS$. The spectrum shows peaks with different intensities at m/z values as illustrated in Scheme 1.

3.6. X ray powder diffraction

The XRD pattern of [Ni(DDPT)(H_2O)(OH)] complex is reported in figure 4 and table 4. All of the diffraction peaks were perfectly indexed into the monoclinic $C_{11}H_{32}N_4NiO_{10}S_2$ structures with lattice constants a=17.0640, b=16.5370, c= 15.3720 Å and α= γ=90 & β= 111.770 º and C 1 2/c space group[41].This is in accordance with the Joint Committee for Powder Diffraction Studies (JCPDS) File No. 26-1342 [41]. Finally, many sharp peaks (at 2θ ≅12.44, 13.21, 15.48, 26.73 29.16, 30.80 and, 36.78º) are appeared in the XRD spectrum attributed to the structural nature of HDDPT ligand meaning that the free ligand of that $Ni(II)^{2+}$ complex presented as semi crystalline form. On the other hand the spectrum of the [Fe (HDDPT) (DDPT)Cl_2]complex (figure 4 & table 5) indexed into an orthorhombic C_{47} Fe_2 N_{19} O_2 S_4 structure with a lattice constants; a=17.1342 Å; b= 17.7157 Å; c= 17.9936 Å and α= γ=90 & β= 111.770 º and P 21 21 21 space group that is in good accordance with the Joint Committee for Powder Diffraction Studies (JCPDS) File No 96-450-9921 [42].

3.7. Thermogravimetric studies

An insight on the data represented (table 6) (figure 5) revealed higher stability on chelation. Thermal degradation takes place through three, two and four steps, respectively. The thermogram of the [Ni(DDPT)(H_2O)(OH)] complex showed first decomposition step at 113-228 °C corresponding to loss of one water molecule (Found: 4.73 %; Calcd.:4. 66 %) which confirmed the existence of water molecules inside the coordination sphere (Figure 5). On the other hand, for example, the TG curve of [Cu (HDDPT) $Cl_2(H_2O)_2$].$2H_2O$ complex exhibited the first decomposition stage at 35-170°C attributed to loss of two water molecules (Found: 8.30%; Calcd.: 7.50%) which evidenced the presence of these molecules as water of crystallization (outside coordination sphere) (Figure 5).The residual part that being left after complete degradation was {MnS, NiS} and CuO+S+3C for present complexes.

3.8. Kinetic data

The kinetic and thermodynamic parameters of thermal degradation process using Coats-Redfern and Horowitz-Metzger models (Supplementary material) (figs. 2S & 3S) [43, 44] have been evaluated. A number of pyrolysis processes can be represented as a first order reaction. The enthalpy of activation, ΔH^*, entropy of activation, ΔS^* and free energy of activation, ΔG^* were calculated by Eyring equation [45].The data obtained are recorded in tables 7 & 8 and represented graphically in. The high values of activation energy, E_a indicates the high stability of chelates because of their covalent bond character [46] and the positive sign of ΔG* indicates all the decomposition steps are non-spontaneous processes and ΔG* increase significantly for the subsequent decomposition stages of a given complex which may be due to increasing the values of TΔS* from one step to another which overrides the values of ΔH* [46]. The values of enthalpy of activation, ΔH^* are positive revealing the degradation process is an endothermic one. On the other hand, ΔS* has negative values indicating more ordered activated complex than the reactants or the reaction is slow [47].

3.9. Computational studies

The DFT molecular modeling structure of HDDPT and its Ni (II) complex are shown in table 9 contains bond lengths and bond angles of DFT optimized structures that are in accordance with analogue compounds with differences { 0.01-0.10 Å} [48,49] that may arise due to the absence of intermolecular interactions between neighboring molecules in gaseous state on applying theoretical calculations for isolated molecules which in contrast the situation is the opposite in solid crystal lattice [49].Table 9 summarizes the variability in the in bond lengths in the five membered chelate ring around Ni(II) species clarifying the significant distortion in the bond angle from optimal square planar environment, i.e., O8-Ni-S10 = 91.43 while O21-Ni-S10 = 96.05 and O22-Ni-O21=83.88°. Also, there is a planarity of the ring system that is maintained on protonation with an apparent bond distance changes occurring mostly in C-S bonds concomitant with smaller changes in C-N bonds. Finally, it is obvious that Ni-O < Ni-S reflecting the high strength of Ni-O bond [50].

The Frontier molecular orbitals (FMO's){ (HOMO and LUMO) }i.e..the highest occupied and lowest unoccupied molecular orbitals that evaluated using B3LYP/6-3111G method are recorded in table 10. For a molecule, the gap between HOMO and LUMO describes the charge transfer and clarifies its chemical stability [51]. Some concepts like chemical reactivity, conjugation, aromaticity and electron lone pair could be obtained molecular orbitals qualitative graphical representation in

which positive is in red and negative is green color [52]. Figure 6 reveals the 3D HOMO and LUMO plots for HDDPT indicating the localization of HOMO;E_{HOMO}=-5.16eV on the thiosemicarbazide arm and the spreading of LUMO; E_{LUMO} = -2.49 eV over the cyclohexane ring as well as thiosemicarbazide moiety with energy gap ΔE = 2.67 eV. For Ni^{2+} complex, FMO's plots (figure 7) indicates the localization of HOMO (-4.06 eV) on phenyl rings and that of LUMO (-2.39 eV) are spreading over the coordinated thiosemicarbazide arm. It is clear that the energy gap ΔE, -1.13 eV of the complex is lower than that of the ligand itself which in turn proves that the present complex could be considered as potential material for harvesting solar radiation in solar cell applications as it can absorb the photons of light beam powerfully increasing the obtained circuit current resulting in more efficient power conversion [53]. The electronegativity (χ) that measure the ability of the molecule to attract electrons and calculated as in literature [45] and that of the ligand (3.82 eV) supporting it behaves as a Lewis acid and that of Ni^{2+} complex (3.50 eV) is extremely low value indicating Lewis base character. Other energetic parameters such as global hardness (η) and global softness (δ) that measure the resistance of a molecule to charge-transfer , and the capability to receive electrons, respectively are recorded in table 10. From the data, one can conclude that Ni^{2+} complex with η = 1.33 and δ = 0.56eV values will be less soft than the thiosemicarbazide, HDDPT [54].

3.10.Corrosion Data

3.10.1.Potentiodynamic polarization (PP) measurements

PP is a useful method because they give more information about the corrosion mechanism and the factors affecting the corrosion process and inhibition behavior of the thiosemicarbazide, HDDPT. The PP has been performed using PCI4-G750 Potentiostat/Galvanostat and a personal computer with Gamry PCI4-G750 software for calculations. In PP measurements, electrode potential from –1000 to 1000 mV was applied at scanning rate 1 mVs^{-1}. %IE and θ from PP measurements from equation:

$$\% \text{ IE} = \theta \times 100 = [(i_{corr\ (free)} - i_{corr(inh)})/ i_{corr\ (free)}] \times 100 \quad (1)$$

where $i_{corr(inh)}$ is the corrosion current density with compound HDDPT and $i_{corr\ (free)}$ is the current without compound HDDPT. PP curves without and with different concentrations for carbon steel dissolution in 1M HCl solution were showed in Figure 8. The difference of corrosion potential (E_{corr}), i_{corr}, β_a, β_c, CR, θ and % IE with compound HDDPT concentration were given in Table11. Experimental results indicate that i_{corr} is significantly decreases with increasing HDDPT

concentration [54]. Both the anodic and cathodic curves were affected by the existence of compound HDDPT, i.e. compound HDDPT limited both the anodic and cathodic reactions (mixed type inhibitor*).* .

3.10.2.Electrochemical Impedance Spectroscopy (EIS) Measurements

EIS tests were utilized to study the mechanism of corrosion. The results of Nyquist and Bode diagrams are demonstrated in Figure 9a, 9b, respectively. These figures indicate a gradual increase in the semicircle diameter of the Nyquist diagrams by raising the concentration of compound HDDPT. So the compound HDDPT retard the corrosion rate by adsorption [55]. From Figure 8a one noticed that the deviation from an ideal semicircle as a result of frequency dispersion because of the inhomogeneity of the surface. Table 12 gives different parameters of impedance as, (R_{ct}), (C_{dl}), (%IE) and electrolyte resistance (R_s). The data of table 10 demonstrated that, the C_{dl} data lowered by raising the concentration of compound HDDPT, this behavior as a result of molecules adsorbed on the surface of carbon steel. Figure 8b shows the equivalent circuit (fig.4S) (Supplementary material) which used in our study [56]. In electrochemical impedance spectroscopy (EIS) procedures, the frequency scope is between 100 kHz and 0.1 Hz and AC signal is 10 mV peak to peak. % IE and θ were obtained by employing the following relation:

$$\%IE = \theta \times 100 = [(R_{ct(free)} - R_{ct(inh)}) / R_{ct(free)}] \times 100 \quad (2)$$

where $R_{ct(inh)}$ is the charge transfer resistance with Compound HDDPT and $R_{ct(free)}$ is the charge transfer resistance without compound HDDPT.

3.11. Antibacterial activity

All compounds under study were screened for inhibition of growth of four bacterial strains, namely *Bacillus* and *Streptococcus pyogenes* (*Strp. py.*) as Gram's positive and *Escherichia coli* (*E.coli*) and *klebsiella spp.* (*kleb. spp.*) as Gram's negative using antibiotics, ampicillin, and ciprofloxacin and gentamicin drugs. The data represented in table1S (Supplementary material) and figure 9 revealed that HDDPT exhibited potent activity against *Strp.py.*) exceeding that of antibiotic itself followed by Co(II), Cu (II) and Ni(II) complexes. HDDPT exhibited potent activity toward Bacillus has the higher activity followed by Cu (II), Co (II) and Ni (II), respectively represented in table 3S (supplementary material) and figure 10. Only Cu (II) has activity against *(kleb. spp.*) while Cu (II) and Co (II) inhibits the growth of E. coli. The inability to inhibit the growth of bacterial strain can be referred to the difficulty of diffusion of the compound through the cell membrane or the possibility

of diffusion through the membrane but being deactivated by unknown cellular mechanism. On the other hand, Cu(II) complex exhibited a higher activity due to the moderate hydrophobicity when compared with HDDPT and other metal complexes resulting in an enhancement of ability to diffuse through the cell membrane and consequently inhibiting the growth of the micro-organisms [57].

3.12. Structure activity relationship (SAR) studies

The potent activity of HDDPT is referred to as its nature as a soft ligand as confirmed by confirmed by the difference between E_{HOMO} and E_{LUMO} (-2.41) in addition to the fact that it contains many free sides, C=O, C=S OH and NH groups free. Also, the reasonable moderate activity of some complexes such as Cu (II) is attributed to the presence of $2Cl^-$ and the smaller size of the metal ion that facilitate the diffusion through the organism membrane.

Conclusion

HDDPT thiosemicarbazide derivative forms new complexes with Mn^{2+}, Fe^{3+}, Co^{2+}, Ni^{2+} and Cu^{2+} ions. Spectral and elemental analyses data suggested an octahedral for all complexes except the diamagnetic Ni^{2+} that adopted a square planar geometry. Also, the ESR data of Cu (II) complex data are consistent with the proposed structure. The higher values ofα^2 and β^2 in case of the complex revealed appreciable covalence in the metal-ligand bonding, presumably arising out of M-thione-coordination. X-ray powder diffraction indicated a monoclinic structure for Ni^{2+} complex and orthorhombic for Fe^{3+} complexes. The TG analysis for the title complexes displayed high residual part indicating high stability of the formed chelates. Moreover, all compounds were screened for antibacterial and antifungal activities. The assay showed a potent activity of the thiosemicarbazide and variable inhibition power for the complexes under study. It was remarked that induction of some moieties, such as an azomethine linkage or a thioketone into a compound causing an extensive biological activities that may be responsible for the increase in the hydrophobic character and liposolubility of the molecules in crossing the cell membrane of the microorganism, thereby enhancing the biological utilization ratio and activity of such complexes**.**

Acknowledgments

First author gratefully acknowledges the Microbiology Unit at Faculty of Pharmacy, Mansoura University, and Mansoura for carrying out the diabetes experimental work.

References

[1] G .A. Gazieva, A. N. Kravchenko "Thiosemicarbazides in the synthesis of five- and six-membered heterocyclic compounds"; Russ. Chem. Rev., (2012) 81 (6) 494 – 523.

[2] X. Zhang, P.lei, T. Sun, X. Jin, X. Yang, Y. Ling" Design, Synthesis, and Fungicidal Activity of Novel Thiosemicarbazide Derivatives Containing Piperidine Fragments "Molecules, (2017)22, 1-13.

[3] P.Meena, V.Nemaysh, M.Khatri, A.Manral, P.M.Luthra, M. Tiwari, "Synthesis, biological evaluation and molecular docking study of novel piperidine and piperazine derivatives as multi-targeted agents to treat Alzheimer's disease" Bioorg. Med. Chem. (2015),23: 1135–1148.

[4] R.M. Lophachin, D.S Barber and T. Gavin. Toxc. Science (2008),104 :235-249.

[5] C. Q. Debra, A. K. Kathy, R. K. Earl, Antiviral Res., (2006), 71, 24.

[6] P. Tarasconi, S. Capacchi, G.Pelosi, M. Cornia, R. Albertini, A. Bonati, P. P. Dall'Aglio, P. Lunghi , S. Pinelli " Synthesis, Spectroscopic Characterization and Biological Properties of New Natural Aldehydes Thiosemicarbazones" Bioorg. & Med. Chem. (2000) ,8 :157-162.

[7] A. Tahghighi, F. B. Thiadiazoles "The appropriate pharmacological scaffolds with leishmanicidal and antimalarial activities": a review; Iran J Basic Med Sci. (2017) 20(6): 613–622.

[8] R. Pingaew, S. Prachayasittikul; S.Ruchirawat "Synthesis, Cytotoxic and Antimalarial Activities of Benzoyl Thiosemicarbazone Analogs of Isoquinoline and Related Compounds" Molecules (2010), 15.

[9] D. Gambino, L. Otero, M. Vieites, M. Boiani, M. Gonzalez, E.J.Baran and H. Cerecetto, "ESR, electrochemical and reactivity studies of antitrypanosomal palladium thiosemicarbazone complexes" Spectrochim. Acta part A, (2008) , 70 :519–523.

[10] O. A. Al-Gammal, A. A. El-Asmy, " Synthesis and spectral characterization of 1-(aminoformyl- N -phenylform)-4-ethylthiosemicarbazide and its metal complexes" J. Coord. Chem., 61, (2008), 2296.

[11] O.A. El-Gammal , G.M. Abu El-Reash ; M.M. El-Gamil .,"Binuclear copper(II), cobalt(II) and Nickel(II) complexes of N1-ethyl-N2-(pyridin-2-yl) hydrazine-1,2-bis(carbothioamide): Structural, spectral, pH-metric and biological studies" Spectrochim. Acta Part A: (2012) , 96,444–455.

[12] O. A. El-Gammal, G. M. Abu El-Reash, M. M. El-Gamil "Binuclear copper (II), cobalt (II) and Nickel (II) complexes of N1-ethyl-N2-(pyridin-2-yl) hydrazine-1,2-bis(carbothioamide): Structural ,spectral, pH-metric and biological studies" Spectrochim. Acta Part A: (2013), 59 -70.

[13] O. A. El-Gammal, G. M. Abu El-Reash, and M. M. El-Gamil " Novel Mercury (II), Cadmium (II) and Binuclear Zinc (II) complexes of N1-ethyl-N2- (pyridine-2-yl) hydrazine-1, 2-bis (carbothioamide): structural, spectral, pH-metric and biological studies" Spectrochim. Acta Part A: (2013),59 -70.

[14] T. A. Yousef, F. A. Badria, Sh. E. Ghazy1, O.A. El-Gammal and G. M. Abu El-Reash "*In vitro* and *in vivo* antitumor activity of some synthesized 4-(2-pyridyl)-3-Thiosemicarbazides Derivatives"., Inter. J. Med.& Med. Sci. (2011) ,3(2),37- 46, .

[15] G. Jeffery, J. Bassett, J. Mendham, R. Denney, Vogel's quantitative chemical analysis, Longman Scientific & Technical Longman Group UK Limited, Essex CM20 2JE, England, (1989).

[16] W.J. Geary, "The use of conductivity measurements in organic solvents for the characterization of coordination compounds", Coord. Chem. Rev. (1971) , 7(1) 81-122.

[17] J.King, "The transferase-alanine and aspartate transaminase in: Practical Clinical Enzymology, Edited by Princeton, M. J., (1965) pp. 363–395. London, Van D Wostrand.

[18] B. Delley" Hardness conserving semilocal pseudopotentials" Phys. Rev.B Cond..Matt., (2002), 66, 155125-155129.

[19] "Modeling and Simulation Solutions for Chemicals and Materials Research", Materials Studio, Version 7.0, Accelrys software Inc., San Diego, USA (2011).

[20] W. J.Hehre, "Ab initio molecular orbital theory", Wiley-Interscience, 1986.

[21]A. Kessi and B.Delley" A scattering theoretic approach to scalar relativistic corrections on bonding"Int. J. Quantum Chem.,(1998),68,135-144.

[22] A.Matveev , M.Staufer,M. Mayer " Density functional study of small molecules and transition-metal carbonyls using revised PBE functionals"; Int. J. Quantum Chem. (1999), 75:863-873.

[23] B.Hammer, L.B.Hansen and J.K.Nørskov" Improved adsorption energetics within density-functional theory using revised Perdew-Burke-Ernzerhof functionals" Phys. Rev. B:Condens. Matter,(1999), 59,7413-7421.

[24] O. A. Al-Gammal, A. A. El-Asmy, ""Synthesis and Spectral Characterization of 1-(aminoformyl-n-phenylform)-4-ethyl Thiosemicarbazide and its Metal Complexes J. Coord. Chem., 61, (2008), 2296--2306.

[25] O.A. El-Gammal and M.M. Mostafa "Synthesis, characterization and molecular modeling of Girard′ T thiosemicarbazide and its complexes with some transition metal ions", Spectrochim. Acta. Part A: (2014), 530-542.

[26] O.A. El-Gammal, G.M. Abu El-Reash; M.M. El-Gamil “Binuclear copper (II), cobalt (II) and nickel (II) complexes of N1-ethyl-N2-(pyridin-2-yl) hydrazine-1,2-bis(carbothioamide): structural, spectral, pH-metric and biological studies”, Spectrochim. Acta Part A: (2012), 96, 444–455.

[27] K. Nakamoto, Infrared and Raman spectra of inorganic and coordination compounds, Wiley Online Library, (1978).

[28] O. A. El-Gammal, G. M. Abu El-Reash, M. M. El-Gamil " Novel mercury (II) cadmium (II) and binuclear zinc (II) complexes of N1-ethyl-N2- (pyridine-2-yl) hydrazine-1, 2-bis (carbothioamide): structural, spectral, pH-metric and biological studies" Spectrochim. Acta Part A: (2013) 59 -70.

[29] O.A. El-Gammal, R.M. El-Shazly, F.E. El-Morsy, A.A. El-Asmy, “Synthesis, characterization, molecular modeling and antibacterial activity of N1′, N2′-bis[1-(pyridin-2-yl) ethylene]oxalohydrazide and its metal complexes” J. Mol. Struct. (2011), 998 .20–29.

[30] N. M. El-Metwally, R. M. El-Shazly, I. M. Gabr, A. A. El-Asmy, Spectrochim. Acta A (2005) 61, 1113-1119.

[31] . J. S.Wood, “Stereochemical and Electronic Structural Aspects of Five-Coordination” Prog. Inorg. Chem. (1971) 16, 227-486.

[32] D.P. Singh, V.B.Rana, “Binuclear chromium(III), manganese(III), iron(III) and cobalt(III) complexes bridged by diaminopyridine” Polyhedron (1995) 14 (20-21) 2901-2906.

[33] A.B.P. Lever, Inorganic Electronic Spectroscopy, Elsevier, Amsterdam, 1984.

[34] T. C. HARROP,P. K. MASCHARAK " Fe(III) and Co(III) Centers with Carboxamido nitrogen and Modified Sulfur Coordination:Lessons Learned from Nitrile Hydratase; Acc. Chem. Res. (2004), 37, 253-260.

[35] C.Y. Su, S. Liao, Y.P. Cai, C. Zhang, B.S. Kang; H.Q. Liu, " Nickel(II) and cobalt(II) complexes with a mixed donor acyclic ligand bearing heterocyclic moieties as terminal groups" Trans. Met. Chem., (2000) 25 (5) 594-598 .

[36] K.A. Ketcham, I. Garcia, J.K. Swearingen, A.K. El-Sawaf, E.Bermejo, A. Castinairas, D.X. West" Spectral studies and X-ray crystal structures of three nickel(II) complexes of 2-pyridineformamide 3-piperidylthiosemicarbazonePolyhedron", (2002), 21(4) 859-865.

[37]S.A.Aly, A.S.Eldourghamy“Synthesis, Characterization of New Copper Complexes of Thiosemicarbazone Derivatives and their Biological Activities" Int. J. Res. Chem. Environ. (2017)7(1) 38-46.

[38] R. P. John, Spectral studies and structure of a 2-hydroxyacetophenone 3-hexamethyleneiminyl thiosemicarbazonate (-2) copper (II) complex containing 1, 10-phenanthroline" Spectrochim. Acta, (2003), 59A (6) 1349- 1358.

[39] K.B. Gudasi, S.A. Patil, R.S. Vadavi, R.V. Shenoy, M. Nethaji, “Crystal structure of 2-[2-hydroxy-3-methoxyphenyl]-3-[2-hydroxy-3-methoxybenzylamino]-1, 2-dihydroquinazolin-4(3H)-one and the synthesis, spectral and thermal investigation of its transition metal complexes, Trans. Met.. Chem. (2006)31(5) 586-592.

[40] D. Kivelson, R. Neiman," ESR studies on the bonding in copper complexes" J. Chem. Phys. (1961)35 (1) 149-155.

[41] R. Sanzenbacher, I. Sotofte, J. Springborg, "Nickel (II) Complexes with [2(4).3(1)] Adam anzane, 1, 4, 7, 10- etraazabicyclo [5.5.3] pentadecane", Acta Chem. Scandinavica, (1999), 53: 457-464.

[42] W. X. Xia, W. Y. You, Y. Pan, X. Y. Yao, H. J. Zhong, D. Bin, W. Ying, W. X. Guang"Synthesis , Structural Variation, an 0064:Characterization of a Series of Crystalline Coordination Compounds with 4-Benzene-1,2,4-triazole:Polymorph, Incomplete Spin Transition, and Single Crystal-to-Single Crystal Trans formation" Crystal Growth & Design (2014) 14(2), 477-490.

[43] A. W. Coats, J. P. Redfern," Kinetic parameters from thermogravimetric data, Nature, (1964), 20(1)68-69.

[44] H. Horowitz, G. Metzger" A new analysis of thermogravimetric traces", Anal. Chem. (1964), 35: 1464 1468.

[45] A. Broido, A simple, sensitive graphical method of treating thermogravimetric analysis data, Journal of Polymer Science Part A-2: Poly. Phys., (1969), 7 : 1761-1773.

[46] R. G. Mortimer "Physical Chemistry" A. Harcourt and Science Technology Company, Academic Press, San Diego, (2000).

[47] S. S. Kandil, G. B. El-Hefnawy, E. A. Baker, Thermal and spectral studies of 5-(phenylazo)-2-thiohydantoin and 5-(2-hydroxyphenylazo)-2-thiohydantoin complexes of cobalt (II), nickel (II) and copper (II), Thermochim. Acta, 414(2004)105-113.

[48] M.R.Mlahi, O.A.El-Gammal, M.H.Abdel-Rhman , I.M. AbdAl-Gader "Synthesis, characterization, DFT molecular modeling and biological studies of Zn (II), Cd (II) and Hg (II) complexes of new polydentate thiosemicarbazide", J.Mol. Struct. (2019) 1182: 168-180.

[49] J. Chocholoušová, V. Špirko, P. Hobza “First local minimum of the formic acid dimer exhibits simultaneously red-shifted O–HO and improper blue-shifted C–HO hydrogen bonds”, Phy. Chem. Chem. Phys., (2004) 6, 37-41.

[50] O.A.El-Gammal, " Synthesis, characterization, molecular modeling and antimicrobial activity of 2-(2-(ethylcarbamothioyl) hydrazinyl)-2-oxo-N-phenylacetamide copper complexes", Spectrochim. Acta Part A: Molecular and Biomolecular Spectroscopy, (2010), 75, 533-542.

[51] S. Xavier, S. Periandy, S. Ramalingam, NBO, "conformational, NLO, HOMO–LUMO, NMR and electronic spectral study on 1-phenyl-1-propanol by quantum computational methods", Spectrochim. Acta Part A: Molecular and Biomolecular Spectroscopy, (2015) 137, 306-320.

[52] V. Arjunan, P. Balamourougane, M. Kalaivani, A. Raj, S. Mohan" Experimental and theoretical quantum chemical investigations of 8-hydroxy-5-nitroquinoline", Spectrochimica Acta Part A: Molecular and Biomolecular Spectroscopy, (2012), 96:506-516.

[53] Ö. Tayfuroğlu, F.A. Kılıçarslan, G.Y. Atmaca, A. Erdoğmuş, Synthesis, characterization of new phthalocyanines and investigation of photophysical, photochemical properties and theoretical studies, J. Porphyrins and Phthalocyanines, (2018), 22: 250-265.

[54] A. S. Fouda, M. Eissa, A. El-Hossiany," Ciprofloxacin as Eco-Friendly Corrosion Inhibitor for Carbon Steel in Hydrochloric Acid Solution " Int. J. Electrochem. Sci., (2018), 13: 11096-11112. .

[55] A.S. Fouda, A. El-Hossiany, H. Ramadan," Calotropis Procera plant extract as green corrosion inhibitor for 304 stainless steel in hydrochloric acid solution" Zastita Materijala (2017), 58(4)541-555.

[56] A.S. Fouda, H. Ibrahim, S. Rashwaan, A. El-Hossiany, R.M. Ahmed," Expired Drug (pantoprazole sodium) as a Corrosion Inhibitor for High Carbon Steel in Hydrochloric Acid Solution" Int. J. Electrochem. Sci.,(2018) 13,6327- 6349.

.

Table 1: Analytical and physical data of HDDPT and its metal complexes.

Compound Empirical formula	F.wt. (Calcd.)	Colour	M.p. (°C)	% Found (Calcd.)						Yield (%)
				M	Cl	C	H	N	S	
HDDPT $C_{15}H_{17}NO_2S$	275.21 (275.37)	White	130	-	-	65.21 (64.21)	6.52 (6.1)	5.23 (5.08)	11.06 (11.64)	85
$[Co(HDDPT)_2Cl_2]$ $C_{30}H_{34}Cl_2CoN_2O_4S_2$	680.38 (680.57)	pale green	240	8.61 (7.90)	10.35 (10.80)	52.89 (52.50)	5.25 (5.00)	4.90 (4.10)	8.92 (9.42)	80
$[Ni(HDDPT)(OH)(H_2O)]$ $C_{15}H_{21}CLNNiO_4S$	366.99 (368.09)	orange	270	15.98 (16.30)	–	48.72 (48.30)	5.91 (5.80)	4.45 (3.78)	8.32 (8.66)	85
$[Cu(HDDPT)Cl_2(H_2O)_2].2H_2O$ $C_{15}H_{25}Cl_2CuNO_6S$	481.04 (481.87)	reddish brown	280	13.15 (14.5)	14.69 (14.20)	37.34 (37.80)	5.32 (5.01)	3.53 (2.90)	6.89 (6.65)	80
$[Mn(DDPT)Cl(H_2O)_3].3H_2O$ $C_{15}H_{28}ClMnNO_8S$	473.21 (472.06)	brown	200	11.50 (10.9)	7.26 (7.40)	38.03 (37.8)	6.14 (5.90)	3.21 (2.97)	7.22 (6.79)	80
$[Fe(HDDPT)(DDPT)Cl_2]$ $C_{30}H_{35}Cl_2FeN_2O_4S_2$	675.42 (676.48)	dark brown	180	8.25 (8.10)	10.4 (11.20)	53.1 (53.02)	5.19 (5.10)	4.67 (4.12)	9.12 (9.44)	82

Molecular weight values obtained from mass spectra.

Table 2: Principle infrared bands of HDDPT and its metal complexes.

Compound	ν(C=O)	ν(O-H)	ν(N-H)	ν(C=S)	δ(C=S)	ν(C=N)*	ν(M-O)	ν(M-S)
HDDPT	1615	3447	3250	1277	785	-	-	-
$[Co(HDDPT)_2Cl_2]$	1625	3432	3150	1347	750	-	524	485
$[Ni(HDDPT)(OH)(H_2O)]$	1607	3447	3061	1270	761	1551	518	490
$[Cu(HDDPT)Cl_2(H_2O)_2].2H_2O$	1624	3473	3160	1275	758	-	513	484
$[Mn(DDPT)Cl(H_2O)_3].3H_2O$	1608	3438	3064	1271	754	1550	504	495
$[Fe(HDDPT)(DDPT)Cl_2]$	1620	3448	3060	1271	757	1553	504	489

Table 3.Magnetic moments and electronic spectral data of HDDPT and its complexes.

Compound	Band position,cm^{-1}	Assignment	Ligand field parameters			μ_{eff} (B.M.)
			B	β	Δ_q	
HDDPT	32580 28370	$\pi \rightarrow \pi^*$ $n \rightarrow \pi^*$	-	-	-	-
$[Co(HDDPT)_2Cl_2]$	15241 20790	$^4T_{1g}(F) \rightarrow {}^4A_{2g}(F)$ $^4T_{1g}(F) \rightarrow {}^4T_{1g}(P)$	964.28	0.993	8148	5.61
$[Ni(HDDPT)(OH)(H_2O)]$	19626 26875	$^1A_{1g} \rightarrow {}^1A_{2g}$ $^1A_{1g} \rightarrow {}^1B_{2g}$	-	-	-	Dia.
$[Cu(HDDPT)Cl_2(H_2O)_2].2H_2O$	19432 21186	$^2B_{1g} \rightarrow {}^2E_g$ $^2B_{1g} \rightarrow {}^2B_{2g}$	-	-	-	2.04
$[Mn(DDPT)Cl(H_2O)_3].3H_2O$	26240 19511 17552	$^6A_{1g} \rightarrow {}^4E_g(^4D)$ $^6A_{1g} \rightarrow {}^4T_{2g}(^4G)$ $^6A_{1g} \rightarrow {}^4T_{1g}(^4G)$	-	-	-	5.64
$[Fe(HDDPT)(DDPT)Cl_2]$	15608 24690 20687	$^6A_{1g} \rightarrow {}^4T_{1g}(G)$ $^6A_{1g} \rightarrow {}^4T_{2g}(G)$ LMCT	-	-	-	4.26

Dia=diamagnetic

Table 4: Powder XRD data: area, FWHM, intensity, crystallite (grain)size D, d-spacing, ε microstrain and dislocation density of $[Ni(HDDPT)(OH)(H_2O)]$complex.

No.	2theta [º]	d [Å]	h,k,l	FWHM	Grain (Cystallite) size D (nm)	Lattice strain ε $x10^{-3}$	Dislocation denisty (A) $x10^{-3}$	Average inner crystal separation (S)
1	7.71	11.45	1,1,0	0.45	18.48	29.1	2.93	14.32
2	12.44	7.11	0,0,2	0.27	30.91	10.8	1.05	8.88
3	13.21	6.70	2,0,-2	0.65	12.85	24.5	6.06	8.37
4	15.48	5.72	2,2,0	0.15	55.82	4.82	3.21	7.15
5	26.73	3.33	5,1,-2	1.15	7.42	21.1	18.2	4.16
6	29.16	3.06	2,4,2	0.45	19.05	7.55	2.75	3.82
7	30.8	2.90	5,3,-2	0.91	9.46	14.4	11.2	3.62
8	31.62	2.83	2,2,4	1.02	8.45	15.7	14.0	3.53
9	36.78	2.44	-116	0.19	46.02	2.49	0.47	3.05
10	40.15	2.24	7,1,0	0.21	42.07	2.51	0.56	2.80
11	41.26	2.19	4,2,4	0.53	16.73	6.14	3.57	2.73
12	43.54	2.08	2,0,6	1.23	7.26	13.4	19.0	2.60
Average	-	4.34	-	0.60	22.88	29.1	6.67	5.42

Table 5: Powder XRD data: area, FWHM, intensity, crystallite (grain)size D, d-spacing, ε microstrain and dislocation density of [Fe (HDDPT) (DDPT)Cl_2] complex.

No.	2theta [º]	d [Å]	hkl	FWHM	Grain (Cystallite) size D (nm)	Lattice strain ε $x10^{-3}$	Dislocation denisty δ (nm^{-1}) $x10^{-3}$	Average inner crystal separation (S)
1	7.06	12.51	1,0,1	0.61	13.71	29.1	2.93	15.63
2	9.72	9.09	0,0,2	0.48	17.35	10.8	1.05	11.36
3	11.00	8.03	0,1,2	0.43	19.39	24.5	6.06	10.04
4	20.00	4.44	0,4,0	0.43	19.59	4.82	0.321	5.54
5	20.37	4.36	0,1,4	0.40	21.08	21.1	18.2	5.44
6	23.52	3.78	4,1,2	0.49	17.30	7.55	2.75	4.72
7	28.24	3.16	0,4,4	0.47	18.20	1.44	11.2	3.95
8	32.62	2.74	4,4,3	0.49	17.64	1.57	14.0	3.43
9	36.20	2.48	1,7,1	0.48	18.19	2.49	0.472	3.10
10	42.56	2.12	3,5,6	0.29	30.71	2.51	0.565	2.65
11	43.01	2.10	0,3,8	0.30	29.73	6.14	3.57	2.63
Average		4.98	-	0.44	20.26	12.7	6.67	6.23

Table 6. Decomposition steps with the temperature range and weight loss for HDDPT and its complexes.

Complex	Temp. Range,°C	Removed species	Wt. Loss	
			Found%	Calcd.%
HDDPT	223-307	$-C_4H_6N + C_5H_7O_2 + H_2S$	73.93	72.83
	308-378	$- C_3H_6$	13.35	14.90
	379-800	3C	12.72	13.07
[Ni(DDPT)(H_2O)(OH)]	113-228	$-H_2O$	4.73	4.66
	229-326	$-H_2O + C_7H_8 + CO_2$	40.86	41.88
	327-507	$-C_7H_5N$	28.88	28.83
	508-800	NiS	25.53	24.63
[Cu (HDDPT) $Cl_2(H_2O)_2$].$2H_2O$	35-170	$-2 H_2O$	8.30	7.50
	171-356	$-2HCL+C_4H_9NO_3$	40.05	40.42
	356-556	$-C_8H_5$	22.29	21.98
	557-800	CuO+S+3C	29.36	30.10
[Mn(DDPT)Cl(H_2O)$_3$].$3H_2O$	25-86	$3 H_2O$	10.46	11.43
	87-266	$3 H_2O$ +HCL	20.28	19.14
	267-465	$CO_2+C_9H_{12}N+5C$	49.82	50.38
	465- 800	MnS	19.41	19.05

Table 7: Kinetic Parameters evaluated by Coats-Redfern equation for HDDPT complexes.

Complex	peak	Mid Temp(K)	Ea KJ/mol	A (S^{-1})	ΔH* KJ/mol	ΔS* KJ/mol.K	ΔG* KJ/mol
[Ni(HDDPT)(OH)(H_2O)]	1st	416.55	25.27	5.03	21.81	-0.2343	119.40
	2nd	599.40	48.25	95.3	43.26	-0.2128	170.83
	3rd	779.64	134.62	$7.14x10^6$	128.13	-0.1217	223.02
[Cu(HDDPT)Cl_2(H_2O)$_2$].2H_2O	1st	375.99	24.50	14.9	19.90	-0.2276	145.83
	2nd	558.04	43.58	50.50	38.94	-0.2175	160.32
	3rd	759.93	96.73	$3.42x10^4$	90.42	-0.1659	216.49
[Mn(DDPT)Cl(H_2O)$_3$].3H_2O	1st	328.56	41.07	$3.76x10^4$	38.34	-0.1581	90.29
	2nd	539.02	65.72	$1.58x10^4$	61.24	-0.1695	152.59
	3rd	737.84	74.66	$5.08x10^3$	68.52	-0.1815	202.44

Table8: Kinetic Parameters evaluated by Horowitz-Metzger equation for HDDPT complexes.

Complex	peak	Mid Temp(K)	Ea KJ/mol	A (S^{-1})	ΔH* KJ/mol	ΔS* KJ/mol. K	ΔG* KJ/mol
[Ni(HDDPT)(OH)(H_2O)]	1st	416.55	32.34	48.70	28.88	-0.2154	118.60
	2nd	599.40	58.22	$8.26x10^2$	53.24	-0.1949	170.04
	3rd	779.64	142.08	$2.27x10^7$	135.60	-0.1121	222.98
[Cu(HDDPT)Cl_2(H_2O)$_2$].2H_2O	1st	375.99	31.07	$1.48x10^2$	27.95	-0.2053	105.14
	2nd	558.04	52.78	$4.24x10^2$	48.14	-0.1998	159.64
	3rd	759.93	108.64	$2.42x10^5$	102.31	-0.1496	216.19
[Mn(DDPT)Cl(H_2O)$_3$].3H_2O	1st	328.56	47.07	$3.78x10^5$	44.33	-0.1390	89.99
	2nd	539.02	75.46	1.54x105	70.98	-0.1505	152.12
	3rd	737.84	88.62	1.10x104	82.49	-0.1751	211.67

Table 9: Selected bond lengths (Å) and bond angles (°) of HDDPT and [Ni(HDDPT)(OH)(H_2O)] complex using DFT-method from $DMOL^3$ calculations.

HDDPT				[Ni(HDDPT)(OH)(H_2O)] complex			
Bond	Length (Å)	Angle	Degree(°)	Bond	Length (Å)	Angle	Degree (°)
N(13)-H(20)	1.019	H(20)-N(13)-C(14)	114.653	O(22)-H(41)	0.991	H(42)-O(22)-H(41)	103.106
N(13)-C(14)	1.425	H(20)-N(13)-C(11)	114.792	O(22)-H(42)	0.986	H(42)-O(22)-Ni(20)	109.792
C(11)-N(13)	1.364	C(14)-N(13)-C(11)	129.502	Ni(20)-O(21)	1.860	H(41)-O(22)-Ni(20)	93.114
C(11)-S(12)	1.682	N(13)-C(11)-S(12)	126.941	O(22)-Ni(20)	2.064	O(21)-Ni(20)-O(22)	83.889
C(4)-C(11)	1.496	N(13)-C(11)-C(4)	116.032	O(8)-Ni(20)	1.990	O(21)-Ni(20)-O(8)	171.782
C(3)-C(4)	1.473	S(12)-C(11)-C(4)	116.954	S(10)-Ni(20)	2.206	O(21)-Ni(20)-S(10)	96.057
C(3)-O(10)	1.245	O(9)-C(5)-C(4)	119.042	S(10)-C(7)	1.800	O(22)-Ni(20)-O(8)	88.609
C(5)-O(9)	1.360	C(11)-C(4)-C(3)	118.824	C(7)-N(11)	1.300	O(22)-Ni(20)-S(10)	179.869
C(4)-C(5)	1.380	C(11)-C(4)-C(5)	121.311	C(4)-C(7)	1.507	O(8)-Ni(20)-S(10)	91.438
C(19)-C(14)	1.410	C(3)-C(4)-C(5)	119.157	C(3)-O(8)	1.411	Ni(20)-S(10)-C(7)	107.532
N(13)-H(20)	1.019	C(4)-C(3)-O(10)	122.061	C(4)-C(5)	1.402	Ni(20)-O(8)-C(3)	112.251
N(13)-C(14)	1.425	C(19)-C(14)	1.410	C(3)-C(4)	1.402	S(10)-C(7)-N(11)	126.683
O(9)-H(31)	0.977	N(13)-H(20)	1.019	O(9)-H(28)	0.983	S(10)-C(7)-C(4)	116.462
C(5)-O(9)	1.360	N(13)-C(14)	1.425	C(7)-N(11)	1.300	N(11)-C(7)-C(4)	116.360
C(4)-C(5)	1.380	O(9)-H(31)	0.977	C(5)-O(9)	1.370	C(7)-C(4)-C(5)	121.731

C(2)-H(21)	1.105	C(5)-O(9)	1.360	C(4)-C(7)	1.507	C(7)-C(4)-C(3)	121.623
C(2)-C(3)	1.530	C(4)-C(5)	1.380	N(11)-C(12)	1.409	C(5)-C(4)-C(3)	116.468

Table 10: Calculated E_{HOMO}, E_{LUMO}, energy band gap ($E_H - E_L$), chemical potential (μ), electronegativity (χ), global hardness (η), global softness (S), global electrophilicity index (ω) and softness (σ) for HDDPT and its complexes.

Compound	E_H / eV	E_L / eV	(E_H-E_L) /eV	χ / eV	μ / eV	η / eV	S / eV^{-1}	ω / eV	σ / eV^{-1}
HDDPT $C_{15}H_{17}NO_2S$	-5.164	-2.491	-2.673	3.8275	-3.8275	1.3365	0.374111485	5.480642069	0.748
$[Co(HDDPT)_2Cl_2]$	-3.142	-2.65	-0.492	2.896	-2.896	0.246	2.032	17.046	4.065
$[Ni(HDDPT)(OH)(H_2O)]$	-4.069	-2.931	-1.138	3.5	-3.5	0.569	0.879	10.764	1.758
$[Cu(HDDPT)Cl_2(H_2O)_2].2H_2O$	-3.823	-3.325	-0.498	3.574	-3.574	0.249	2.008	25.649	4.016
$[Mn(DDPT)Cl(H_2O)_3].3H_2O$	-3.14	-2.185	-0.955	2.662	-2.662	0.477	1.047	7.423	2.094
$[Fe(HDDPT)(DDPT)Cl_2]$	-3.737	-3.400	-0.337	3.568	-3.568	0.1685	2.967	37.786	5.934

H=HOMO, L=LUMO.

Table 11. The effect of compound (HDDPT) concentrations on the free corrosion potential (E_{corr}), corrosion current density (j_{corr}),,Tafel slopes(β_c ,β_a), degree of surface coverage (θ) ,inhibition efficiency(%IE) and corrosion rate(CR) of 1 M HCl at 25°C.

C_{inh}, M	$-E_{corr}$, mV vs SCE	i_{corr}, μA cm^{-2}	β_c, mV dec^{-1}	β_a, mV dec^{-1}	CR, mmy^{-1}	□	% IE
Blank	399	128.0	109	94	85.2	—	—
$1x10^{-6}$	394	69.80	107	86	32.6	0.457	45.7
$5x10^{-6}$	393	48.90	110	79	28.6	0.623	62.3
$10x10^{-6}$	397	30.60	108	76	13.9	0.768	76.8
$15x10^{-6}$	400	15.60	86	62	7.5	0.881	88.01

Table 12**.** EIS results without and with different compound (HDDPT) concentrations for carbon steel in corrosive solution.

Compounds	Concentration M	$C_{dl}x10^{-3}$, μF cm^{-2}	R_{ct}, Ω cm^2	θ	% IE
Blank	0.0	5.60	5.68	----	----
HDDPT	$1x10^{-6}$	4.30	7.40	0.233	23.3
	$5x10^{-6}$	2.80	13.07	0.565	56.5
	$10x10^{-6}$	2.10	14.80	0.616	61.6
	$15x10^{-6}$	1.80	19.24	0.705	70.5

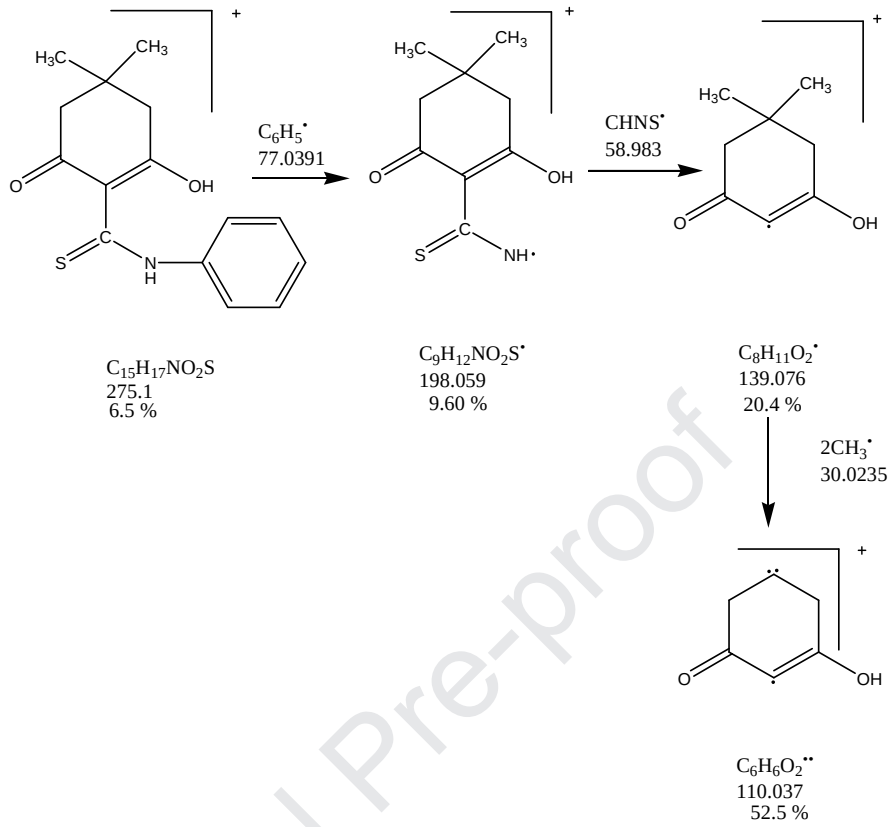

Scheme 1: fragmentation pattern of HDDPT.

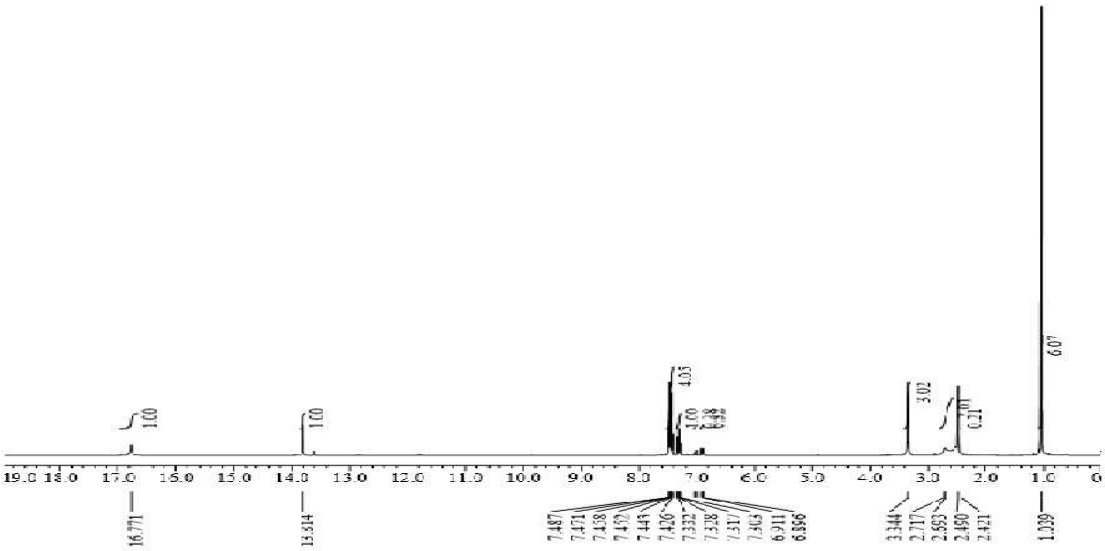

(a)

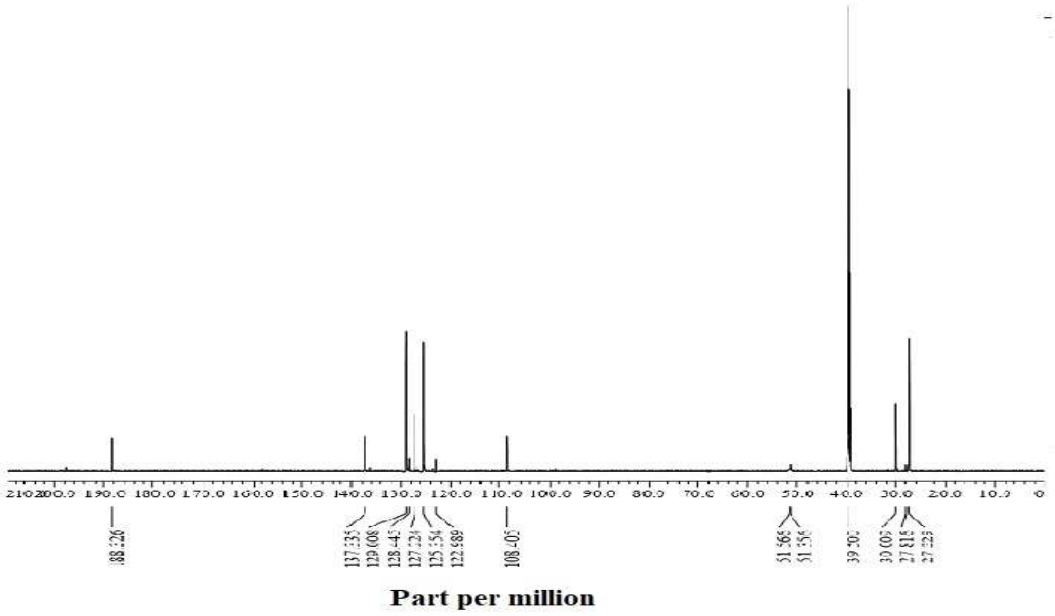

(b)

Figure 1: (a) ^{1}HNMR and (b) ^{13}CNMR spectra of HDDPT in d_6DMSO.

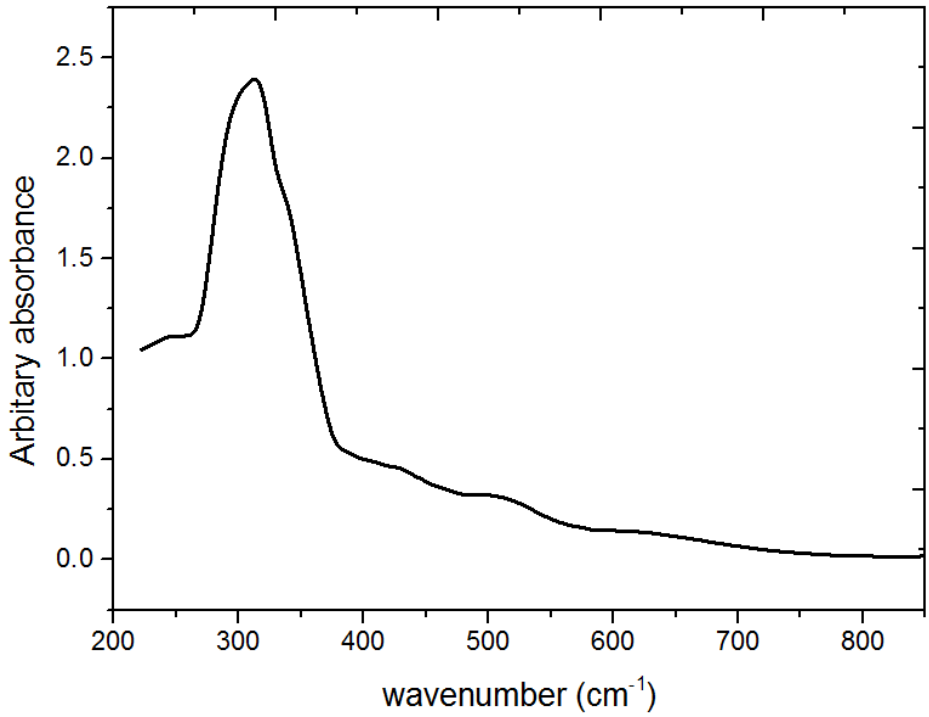

Figure 2. Electronic spectrum of [Ni(DDPT)(OH)(H_2O)] complex.

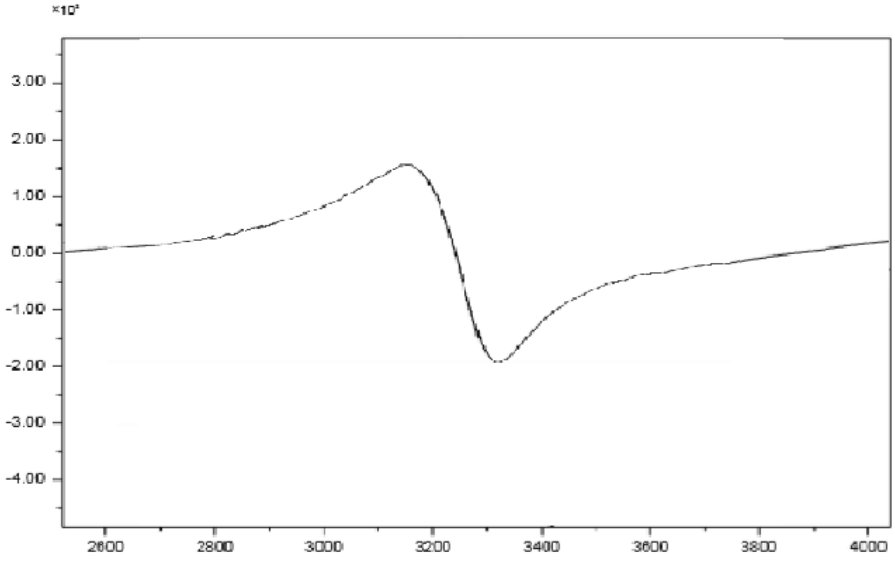

Figure 3, ESR spectrum of [Cu(HDDPT)Cl_2].4H_2O complex

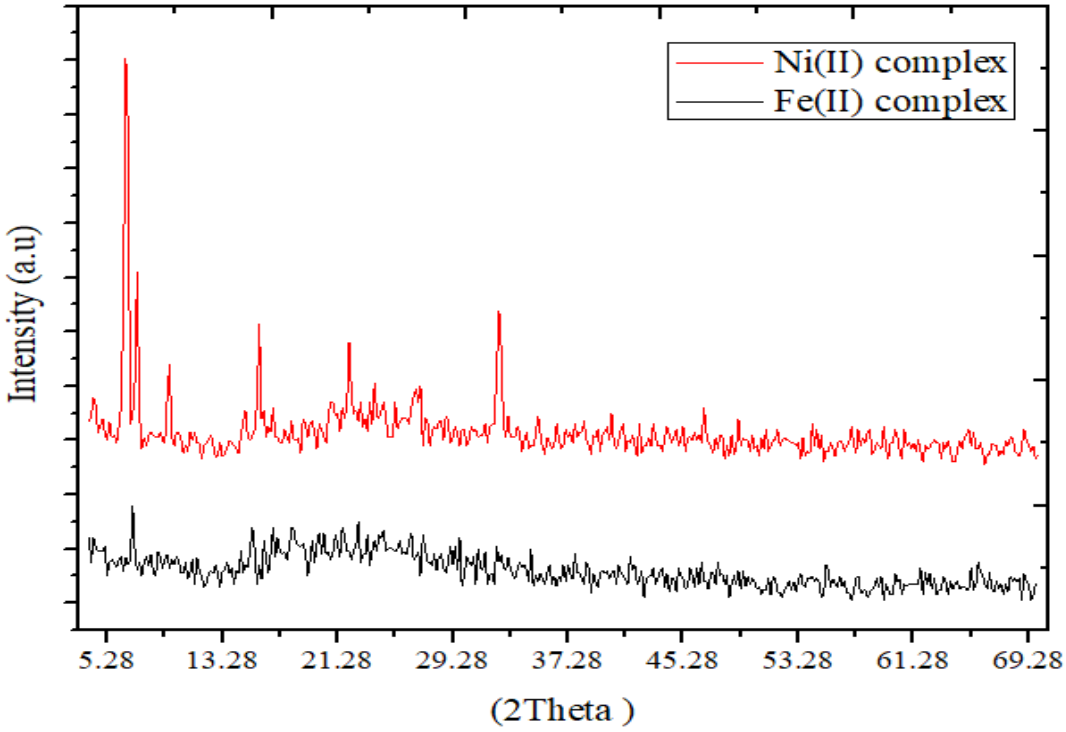

Figure 4.x-ray powder diffraction spectrum of [Fe(HDDPT)(DDPT)Cl_2] and [Ni(DDPT)(OH)(H_2O)] complexes.

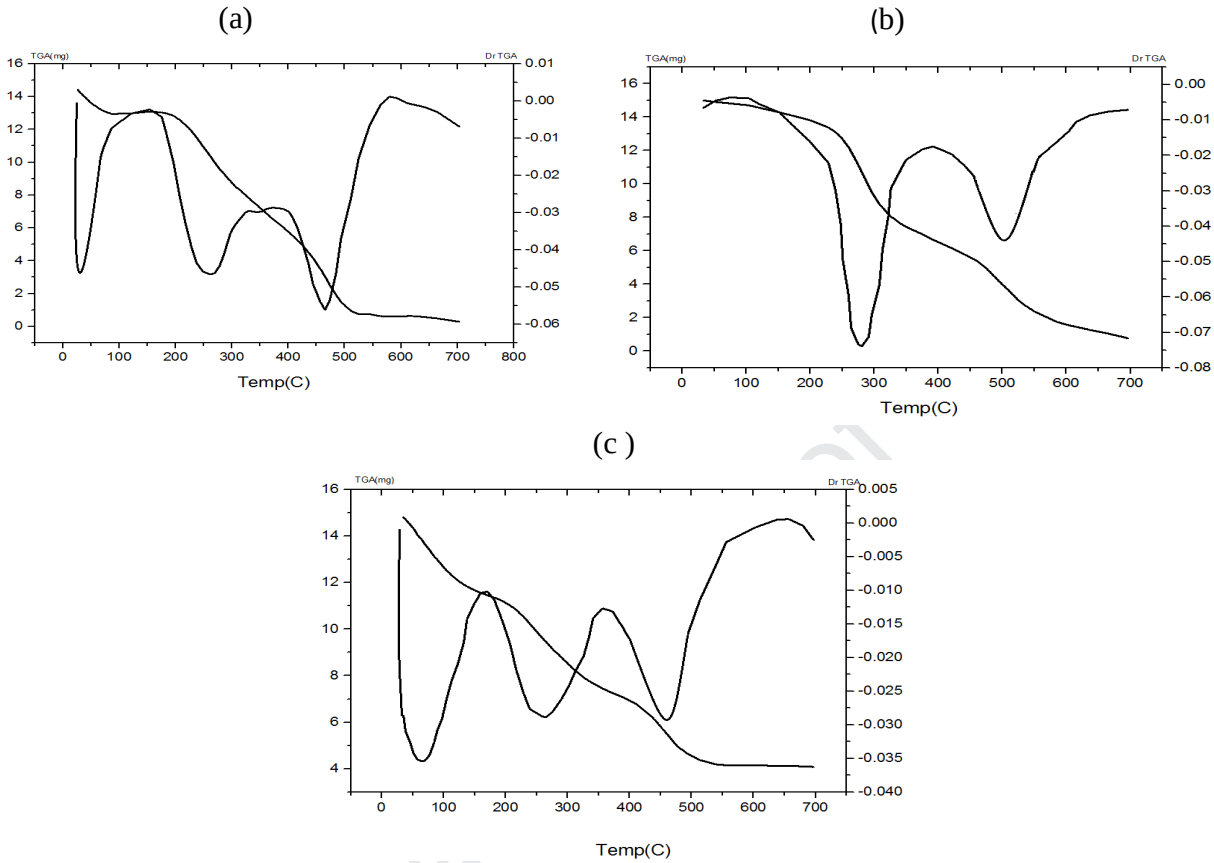

Figure 5.TGA curves of: (a) $[Mn(DDPT)Cl(H_2O)_3].3H_2O$ (b) $[Ni(DDPT)(OH)(H_2O)]$ and (c) $[Cu(HDDPT)Cl_2(H_2O)_2].2H_2O$ and complexes.

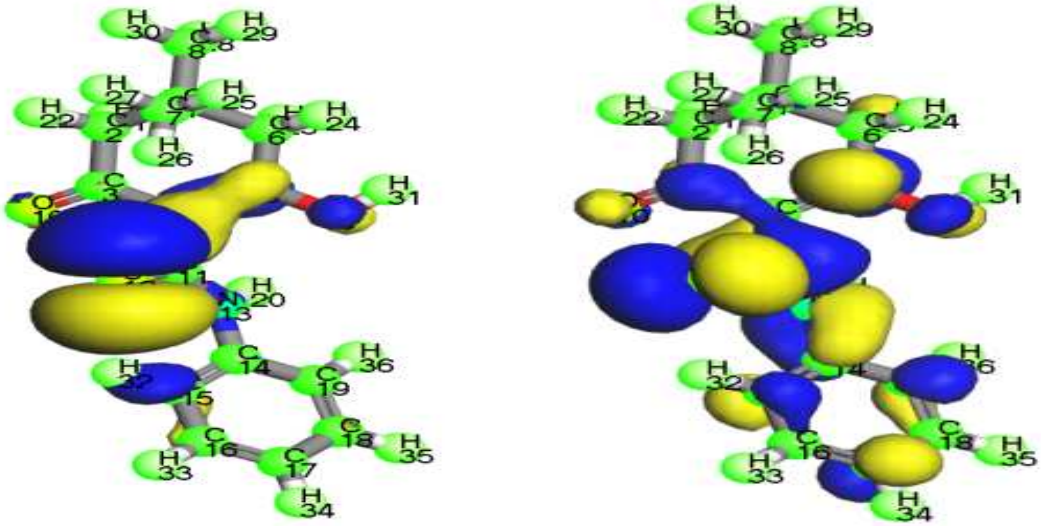

(a) (b)

Figure 6: (a) HOMO and (b) LUMO of HDDPT.

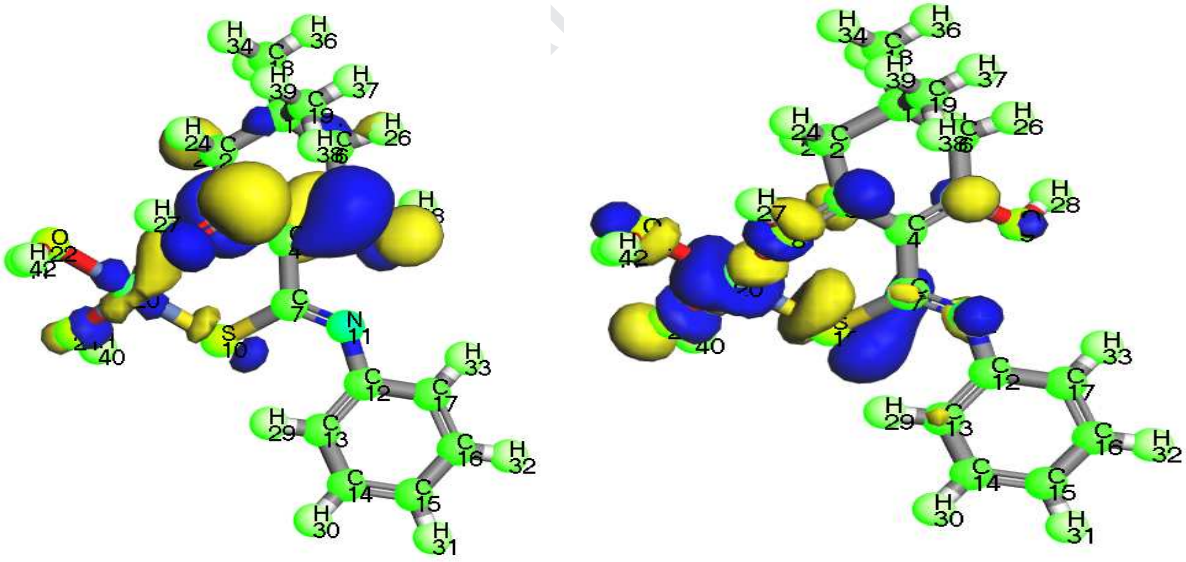

(a) (b)

Figure 7: (a) HOMO and (b) LUMO of [Ni(DDPT)(OH)(H_2O)].

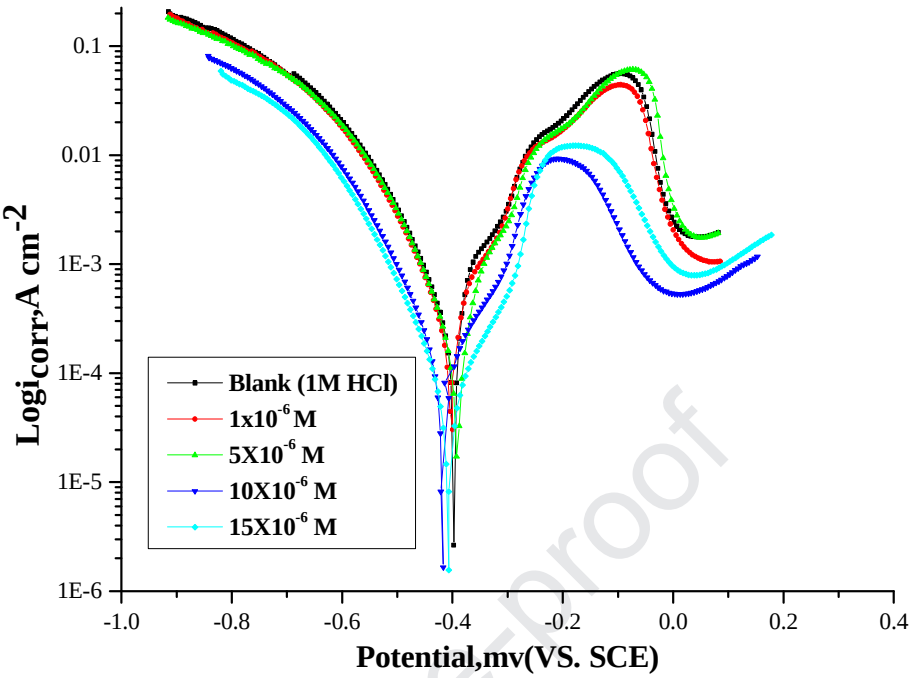

Figure 8. PP curves for carbon steel dissolution of 1M HCl in the absence and presence of different concentrations of compound (HDDPT) at 25^{o}C .

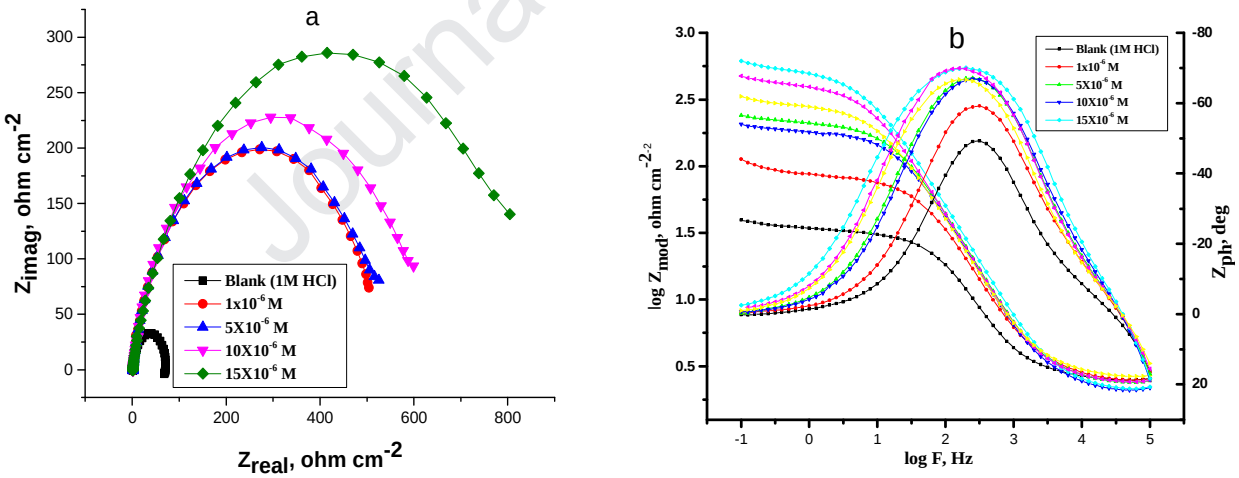

Figure 9. (a) EIS Nyquist and (b) Bode plots for 1 M HCl in the absence and presence of different concentrations of compound (HDDPT) at 25^{o}C.

.

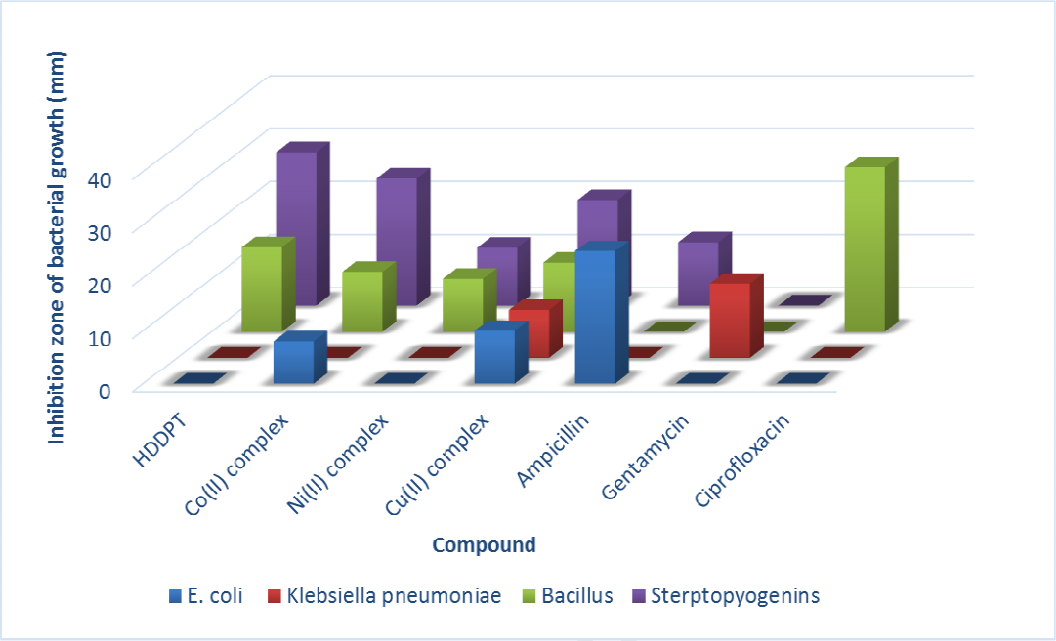

Figure 10. Comparison of inhibition zone (in mm) of HDDPT and its complexes against Gram-positive and gram negative.

Highlights

- Preparation of Mn^{2+}, Fe^{3+}, Co $^{2+}$, Ni $^{2+}$ and Cu^{2+}complexes of a new thiosemicarbazide.
- Elemental analysis, spectral characterization of the ligand and complexes.
- Thermal behavior of the solid metal complexes was studied using TGA technique.
- Antibacterial and corrosion inhibition of the ligand towards carbon steel was examined.

1. The student, Doha Nabih has carried out the experimental work.

2. Prof.Dr. Abdelaziz E.Fouda has interpreted the part of corrosion study.

3. The corresponding author; Prof.Dr.Ola suggested the point of research, plan of work, interpreted the characterization part including elemental, spectral , molecular modelling, X-ray and biological study and write the research and submitted the research to the journal.

The title compounds were screened for *in vitro* antibacterial and the corrosion hindrance of carbon steel metal in 0.5M HCl by HDDPT was tested utilizing potentiodynamic polarization. The ligand under investigation has not been undertaken. Accordingly, a study of new thiosemicarbazide as well as its some transition metal complexes with antibacterial inhibition would support the development of new drugs and improve the treatment of various diseases. In addition, its inhibition towards the corrosion of carbon steel may facilitate its development in steel products industry to maintain the metal hardness.